Solidification of Neutron Matter

V. Canuto* and S. M. Chitre†
Institute for Space Studies, National Aeronautics and Space Administration, Goddard Institute for Space Studies, New York, New York 10025
(Received 10 January 1973)

A t-matrix calculation of the ground-state energy of cold neutron matter has been performed and it is shown that neutron matter solidifies at a density of the order of 1.6×10^{15} g/cm^3, thus implying the existence of a solid core inside heavy neutron stars.

There has been a growing interest recently in the existence of a solid core inside neutron stars, a possibility which appears to be observationally supported by repeated speedups recorded in the Vela pulsar.[1] There have been four reported calculations to establish whether a system of baryons could solidify in the range of densities of interest in neutron stars, i.e., $5\times10^{14} \leq \rho \leq 10^{16}$ g/cm^3.

Anderson and Palmer,[2] on the basis of de Boer's law of corresponding states, first indicated that solidification would indeed occur at $\rho = 5\times10^{14}$ g/cm^3, a result that was not significantly altered by a refined version by Clark and Chao.[3] Then Nosanow and Parish,[4] using a Monte Carlo technique analogous to the one used for solid He^3, found the onset of a neutron solid state at $\rho \cong 3 \times 10^{14}$ g/cm^3. Lastly, Pandharipande[5] performed a variational computation that indicates that neutrons do not solidify until 3.34×10^{15} g/cm^3.

In this paper we report the results of a t-matrix computation that indicates the onset of the solid phase at $\rho \sim 1.6\times10^{15}$ g/cm^3.[6] Such an approach has been successfully employed in the description of solid He^3.[7] Our earlier attempts to use variational methods as in Refs. 3 and 4 fell short of a satisfactory treatment of the angular-momentum– and spin-dependent character of nuclear forces. Up to second order, the energy per particle is known to be[7]

$$E/N = \tfrac{3}{4}\hbar\omega + \tfrac{1}{2}\textstyle\sum_{ij}\int \Phi_{ij} V_{ij} \psi_{ij}\, dr_i\, dr_j , \tag{1}$$

where Φ_{ij} is the two-body uncorrelated wave function which is the product of two Gaussian functions centered at the lattice sites $\vec{R}_i$ and $\vec{R}_j$, respectively,[7] i.e.,

$$\Phi_{ij} = \varphi(i)\varphi(j) = \Phi(\vec{R})\varphi(\vec{r}) = \frac{\alpha^{3/2}}{(\pi/2)^{3/4}} \exp[-\alpha^2(\vec{R}-\vec{\Delta})^2] \frac{\alpha^{3/2}}{(2\pi)^{3/4}} \exp[-\tfrac{1}{4}\alpha^2(\vec{r}-\vec{\delta})^2], \tag{2}$$

with $(\vec{\delta}, 2\vec{\Delta}) = \vec{R}_i \mp \vec{R}_j$ and $\alpha = (m\omega/\hbar)^{1/2}$; ψ_{ij} is the correlated two-body wave function that is taken to satisfy the Bethe-Goldstone equation,[7]

$$[T(i)+T(j)+U(i)+U(j)+V_{ij}]\psi_{ij} = \epsilon\psi_{ij}, \tag{3}$$

where the self-consistent one-body potentials U are given by

$$\varphi(i)U(i)\varphi(i) = \textstyle\sum_j \int \varphi(i)\varphi(j) V_{ij}\psi_{ij}\, dr_j . \tag{4}$$

The frequency of oscillation ω is obtained by solving the set of equations (1)–(4) simultaneously. After separating center of mass and relative coordinates, Eq. (3) reduces to $[\psi_{ij} = \Phi(\vec{R})\psi(\vec{r})]$,

$$[-(\hbar^2/m)\nabla_r^2 + \tfrac{1}{4}m\omega^2(\vec{r}-\vec{\delta})^2 + V(\vec{r})]\,\psi(\vec{r}) = (\epsilon - \tfrac{3}{2}\hbar\omega)\psi(\vec{r}). \tag{5}$$

The wave function ψ has to be taken dependent upon M_S, the projection of the total spin S, since the energy depends upon the spin configuration used in the crystal structure under consideration. We will in fact specify the lowest-energy configuration by arranging the spins in a specific order. It is obvious that a configuration with all spins parallel will yield too much energy because of the presence of $^3P_1$ which is always repulsive at any distance. (We have used the Reid potential.) The general wave function is therefore written as [see Eq. (6.3) of Bethe, Brandow, and Petschek[8]]

$$\psi^{SM_S}(\vec{r}) = \textstyle\sum_{lJ} i^l [4\pi(2l+1)]^{1/2} (l0SM_S|\, JM_S)\psi_{lJ}^{M_S}(r) Y_{lJ}^{M_S}(\Omega). \tag{6}$$

After considering the three possibilities (a) $S=0$, $M_S=0$, (b) $S=1$, $M_S=0$, (c) $S=1$, $M_S=1$, and substituting the three resulting wave functions in Eq. (5), we get three sets of coupled differential equa-

tions. The coupling of various waves (within a prescribed spin configuration) is due to the term $\vec{r}\cdot\vec{\delta} = r\delta\cos\theta$ that couples odd and even waves. We had originally worked out the problem including waves up to $l=2$.[6] Following a remark by Bethe, we have extended the computation up to $l=4$ and subsequently up to $l=6$. The $l=4$ gave lower energy than the $l=2$ case, whereas we found little difference between $l=4$ and $l=6$.

Since for triplet states $|l-1| \leq J \leq l+1$, the $S=1$ ($M_S=0,1$) states give rise respectively to 13 and 18 equations with $l \leq 6$. Even though the energy was sensibly unaltered from say $l=4,5$, we extended the triplet waves to include $l=7$. On the other hand, the singlet states, for which $l=J$, can be extended up to $l=25$ without any problem. This was also done with hardly any change in the final result. As for the potentials, we used for higher l's an approximation suggested to us by Bethe[6]: $V(l=\text{even}) = V(^1D_2)$, $V(l=\text{odd}) = V_c(^3P_2 - {}^3F_2)$, $l \geq 3$. The choice $V(l \geq 3) = 0$ was also employed. For both cases the results were essentially unaltered. Even though we cannot claim that $l_{\max}$ taken here is the right one, we feel, however, that a reasonable convergence has been achieved.

The three sets of equations for the cases (a), (b), and (c) contain respectively 7, 13, and 18 coupled differential equations each, for a total of 38 partial waves ($^1S_0 \cdots {}^1I_7$; $^3S_1 \cdots {}^3I_7$;).

(a) $S=0$, $M_S=0$. In this case, the inclusion of $l=6$ waves gives rise to 7 coupled equations that are written in the following concise form:

$$F_l{}^{J\prime\prime} + (E - U_l{}^J)F_l{}^J + \frac{(-1)^{l+1}}{2l+1}\frac{a^4xd}{2}[lF_{l-1}{}^{J-1} - (l+1)F_{l+1}{}^{J+1}] = 0$$

($l=0,\ldots,6$) and $l=J$.

(b) $S=1$, $M_S=0$.

$$G_l{}^{J\prime\prime} + (E - U_l{}^J)G_l{}^J + \frac{(-1)^{l+1}}{2l+1}\frac{a^4xd}{2}[l\textstyle\sum_{J'}(l+1010|J'0)^2 G_{l+1}{}^{J'} - (l+1)\sum_{J''}(l-1010|J''0)^2 G_{l-1}{}^{J''}] = 0$$

($l=0,\ldots,6$) and J takes the values compatible with $|l-1| \leq J \leq l+1$, and likewise the sum over J' and J'' follows the rule $|l| \leq J' \leq l+2$, $|l-2| \leq J'' \leq l$.

(c) $S=1$, $M_S=1$.

$$H_l{}^{J\prime\prime} + (E - U_l{}^J)H_l{}^J + \frac{(-1)^{l+1}}{2l+1}\frac{a^4xd}{2}[l\textstyle\sum_{J'}(l+1011|J'1)^2 H_{l+1}{}^{J'} - (l+1)\sum_{J''}(l-1011|J''1)^2 H_{l-1}{}^{J''}] = 0.$$

The notation is as follows:

$$U_l{}^J = \tfrac{1}{4}a^4x^2 + (mr_0{}^2/\hbar^2)V_l{}^J + l(l+1)/x^2, \quad F_l{}^J, G_l{}^J, H_l{}^J = r\psi_l{}^J,$$

$$E = (mr_0{}^2/\hbar^2)[\epsilon - \tfrac{3}{2}\hbar\omega - (\hbar^2/4m)\alpha^4\delta^2 - 2U_0], \quad a = \alpha r_0, \quad x = r/r_0, \quad d = \delta/r_0,$$

$$\rho = m\gamma/r_0{}^3 \quad (\gamma = 4, \text{ fcc}; \ \gamma = 2, \text{ bcc}).$$

Once the ψ's are known for each spin and angular-momentum component, the energy can readily be computed by using Eq. (1). The wave function ψ for the $^1S_0$ state is shown in Fig. 1 along with the unperturbed wave function φ and the correlation function $f(r) = \psi/\varphi$. The computation of the wound parameter κ turns out to be $\lesssim 0.25$.

Even though a bcc structure yields lower energy than fcc for the first shell, the second and third shells both have spins $\uparrow\uparrow$ for bcc and $\uparrow\downarrow$ for fcc. The fourth shell again favors bcc, but the fifth and sixth favor favor fcc. The situation repeats until one finds a net gain with an fcc structure of about 30 MeV at $\rho = 3.34\times10^{15}$ g/cm^3.

In the range $1.6\times10^{15} \lesssim \rho \lesssim 5\times10^{15}$ g/cm^3 the spread of the single-particle wave function turns out to be $0.238 \lesssim \alpha^{-1} \lesssim 0.333$ F, whereas the first-neighbor distance is $0.779 \lesssim \delta \lesssim 1.139$ F. The plot of E/N versus ρ for fluid[9] and solid configurations is displayed in Fig. 2, where we include the results of the early computation with only $l=0,1,2$. It is concluded that from $\rho = 1.6\times10^{15}$ g/cm^3 the solidlike arrangement gives a lower energy per particle than the fluid. However, since the fluid energy has been computed variationally, it represents an upper limit and therefore the present computation can only be taken to indicate that there is a good chance for a solid phase at high density, but not a definite proof.

A remark about higher-order terms is appro-

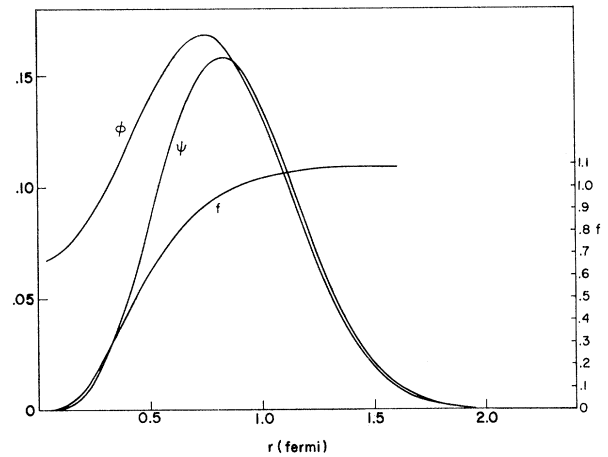

FIG. 1. Wave function ψ for the singlet state $^1S_0$ along with the correlation function f and the unperturbed wave function φ for the same state at $\rho = 3.34\times10^{15}$ g/cm^3. The nearest-neighbour distance $\Delta = 0.891$ F.

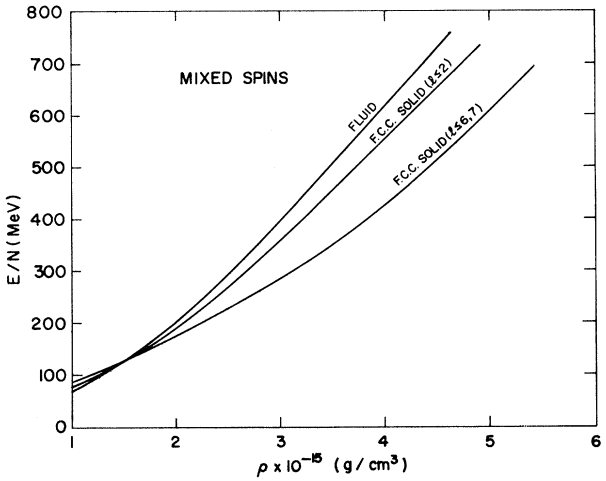

FIG. 2. Ground-state energy per particle versus the density for a neutron fcc lattice and neutron fluid. Results of earlier computation with $l \leq 2$ are displayed for comparison.

priate. In systems that are translationally invariant the unperturbed wave functions are usually taken to be plane waves. Solid hydrogen has recently been studied by Ostgaard,[10] and Eq. (1) was found to work surprisingly well. This is partly because instead of plane-wave single-particle wave functions, the choice appropriate to a translationally invariant system, one employs Gaussian wave functions, which already incorporate some higher-order correlations. Furthermore, the wound parameter κ, whose size measures the importance of three-body correlations, turns out to be only about 0.2.

The method outlined in this paper has been applied to He^3 and solid hydrogen, and the results are in satisfactory agreement with experimental data.[11]

Once the energy per particle E/N is known, it is a simple matter to compute the energy density and the pressure. We have fitted the pressure P versus the mass-energy density ϵ with a polynomial expression in the density range $1.6\times10^{15} \leq \rho \leq 6\times10^{15}$ g/cm^3:

$$P_{36} = 0.205\,79 - 0.271\,60\epsilon_{36} + 0.181\,809\epsilon_{36}^2 - 0.008\,803\,7\epsilon_{36}^3,$$

where

$P_{36} = P\times10^{-36}$ dyne/cm^2;

$\epsilon_{36} = \epsilon\times10^{-36}$ erg/cm^3.

For densities lower than 1.6×10^{15} g/cm^3, our P and ϵ join smoothly the equation of state given by Pandharipande.[9] We integrated the general relativistic equations of hydrostatic equilibrium and found the mass upper limit for a stable neutron star to be $1.39M_\odot$ at $\rho = 4\times10^{15}$ g/cm^3.

Finally, a comparison with the previous computations[4,5] is in order. In the Monte Carlo computation, the correlation function was chosen to be of the form $f = \exp(-b/r^n)$ with $n = 4$, which appears to be rather different from the one obtained either by us or by Pandharipande. Moreover, the nucleon-nucleon interaction was drastically simplified in order to make the computation managable. Such a simplification may be justifiable at low density, but it surely becomes questionable as the density increases. The rather low solidification density is probably a result of the choice of the correlation function.

In Ref. 5, the variational computation was supplemented by Eq. (5) for ψ. The important $\vec{r}\cdot\vec{\delta}$ term that couples all the waves was averaged and no angular-momentum expansion of the wave function was performed. In our approach one major concern was the state-dependent correlation function which was exactly treated. In the opinion of the present authors the healing conditions used in Ref. 5 are too restrictive (the f has no overshoot). In particular, an f restricted to be ≤ 1 for any r does not seem to be able to satisfy the normalization condition $\int\psi\varphi\, d^3r = \int\varphi^2 f \times d^3r = 1$, if φ is taken to be a Gaussian wave function normalized to unity.

Finally, there is an astrophysical piece of evidence to support the idea of a solid core inside heavy neutron stars. This relates to the fact that

the starquake theory of pulsar speed-ups, which can plausibly account for the behavior of the Crab pulsar, can also explain the observed features of the Vela pulsar only if it is assumed that the Vela possesses a solid core. Pines, Shaham, and Ruderman[1] have argued that the solid core has sufficient elastic energy to power the starquakes of the magnitude and frequency in the Vela pulsar.

The authors would like to express their gratitude to Dr. H. A. Bethe for valuable criticism of our earlier computation. It is also a pleasure to thank B. Brandow, A. G. W. Cameron, L. Nosanow, V. R. Pandharipande, and M. Ruderman for their interest and helpful comments.

[1]D. Pines, J. Shaham, and M. Ruderman, Nature (London) 237, 83 (1972).

[2]P. W. Anderson and R. G. Palmer, Nature (London) 231, 145 (1971).

[3]J. W. Clark and N. C. Chao, Nature (London) 236, 37 (1972).

[4]L. Nosanow and L. Parish, in Proceedings of the Sixth Texas Symposium on Relativistic Astrophysics, New York, December 1972 (New York Academy of Sciences, to be published).

[5]V. R. Pandharipande, in Proceedings of the Sixth Texas Symposium on Relativistic Astrophysics, New York, December 1972 (New York Academy of Sciences, to be published).

[6]V. Canuto and S. M. Chitre, in Proceedings of the International Astronomical Union Symposium on the Physics of Dense Matter, Boulder, Colorado, 1972 (to be published).

[7]B. H. Brandow, Ann. Phys. (New York) 74, 112 (1972). R. A. Guyer and L. I. Zane, Phys. Rev. 188, 445 (1969). F. Iwamato and H. Namaizawa, Progr. Theor. Phys. 45, 682 (1971).

[8]H. A. Bethe, B. H. Brandow, and A. G. Petschek, Phys. Rev. 129, 225 (1963).

[9]V. R. Pandharipande, Nucl. Phys. A174, 641 (1971).

[10]E. Ostgaard, Z. Phys. 252, 95 (1942).

[11]V. Canuto, S. M. Chitre, and J. Lodenquai, to be published.

*Also with the Department of Physics, The City College of the City University of New York, New York, N. Y. 10031.

†On leave of absence from the Tata Institute of Fundamental Research, Bombay, India.

Muon Polarization in the Decay $K_L^0 \to \pi^- \mu^+ \nu_\mu$, an Experimental Test of Time-Reversal Invariance*

J. Sandweiss, J. Sunderland, W. Turner, and W. Willis
Yale University, New Haven, Connecticut 06520

and

L. Keller†
Argonne National Laboratory, Argonne, Illinois 60439

(Received 8 January 1973)

We report the results of a high-statistics scintillation-counter electronics experiment measuring the muon polarization in the decay $K_L^0 \to \pi^- \mu^+ \nu_\mu$ by the method of spin precession. We present results for the real and the imaginary parts of the form-factor ratio.

CP noninvariance is well established in the neutral-kaon system. Time-reversal noninvariance is implied, but has never been directly observed.[1] In the K_L^0 c.m. system a component of muon polarization normal to the decay plane $(\vec{\sigma}_\mu \cdot \vec{P}_\pi \times \vec{P}_\mu)$ in $K_L^0 \to \pi^- \mu^+ \nu_\mu$ is odd under time reversal T and forbidden by T invariance.[2] In this Letter we report the results of an attempt to observe T noninvariance directly by measurement of muon polarization in the decay $K_L^0 \to \pi^- \mu^+ \nu_\mu$.

Briefly, our experimental technique is to record in plastic scintillation counters a prompt coincidence signifying π^- and μ^+ from in-flight $K_L^0 \to \pi^- \mu^+ \nu_\mu$ decay, degrade the muon to rest, and record a delayed coincidence signifying the e^+ preferentially emitted along the polarization vector of μ^+ in the decay $\mu^+ \to e^+ \nu_e \bar{\nu}_\mu$. To measure the muon polarization we have used the method of spin precession, recording the time distribution of the e^+ from μ^+ precessing in a 60-G magnetic field (1.8 turns per μ^+ lifetime) superimposed on the μ^+ stopping volume. The phase and magnitude of the observed sinusoidal modulation of the μ^+ decay intensity are directly